J. Fluid Mech. (1982), *vol.* 115, *pp.* 1–11
Printed in Great Britain

Where to put a steady discharge in a river

By RONALD SMITH

Department of Applied Mathematics and Theoretical Physics,
University of Cambridge, Silver Street, Cambridge

(Received 8 July 1981)

To avoid high pollution levels along the banks of a river it is desirable to site steady discharges somewhere near the centre of the stream. Here it is shown that the precise location of the optimal discharge site is at the single zero crossing of the first advection–diffusion eigenmode. Simple examples reveal that this position tends to be weighted towards the deeper parts of the channel, and towards the inside bank at the beginning of bends.

1. Introduction

To alleviate water-pollution problems large-scale industrial processes and sewage works are designed to avoid sporadic high-level discharges, and instead are aimed at steady low-level discharges. In confined waterways this means that far downstream of the outlet the contaminant load will have become distributed evenly throughout the flow.

The position of a single discharge point, or the distribution of multiple discharges, determines the way in which the asymptotic state is approached. The most ambitious target would be to minimize the peak concentration anywhere in the flow. This can be achieved if the discharge rate at each point across the flow is exactly matched to the local volume flow rate, i.e. the constant-concentration asymptote is attained immediately.

A more practicable target is to restrict attention to a single discharge point and to minimize the peak concentration at the shoreline, e.g. with the objective of minimizing the risk of infection for animals foraging along the banks. If the discharge site were too near one of the banks then the contaminant plume would reach that bank relatively soon with a concentration in excess of the eventual asymptote (figure 1). In a straight channel with a symmetric depth profile the shoreline concentration would exhibit such an overshoot unless the outlet were positioned at the centre. Thus, the question being asked here amounts to: 'where is the centre of a non-symmetric or meandering river?'.

For river life shoreline concentrations are unimportant. However, it is desirable that the zone of high concentrations be of small extent. Yotsukura & Cobb (1972; figures 13, 14) used the degree of mixing as a measure of the effectiveness of different discharge locations. Fortuitously, the definition used in the present paper for the best discharge site is equivalent to requiring that complete mixing is achieved as quickly as possible. For sudden discharges the appropriate considerations, and the optimal discharge locations, are quite different (Smith 1981*a*).

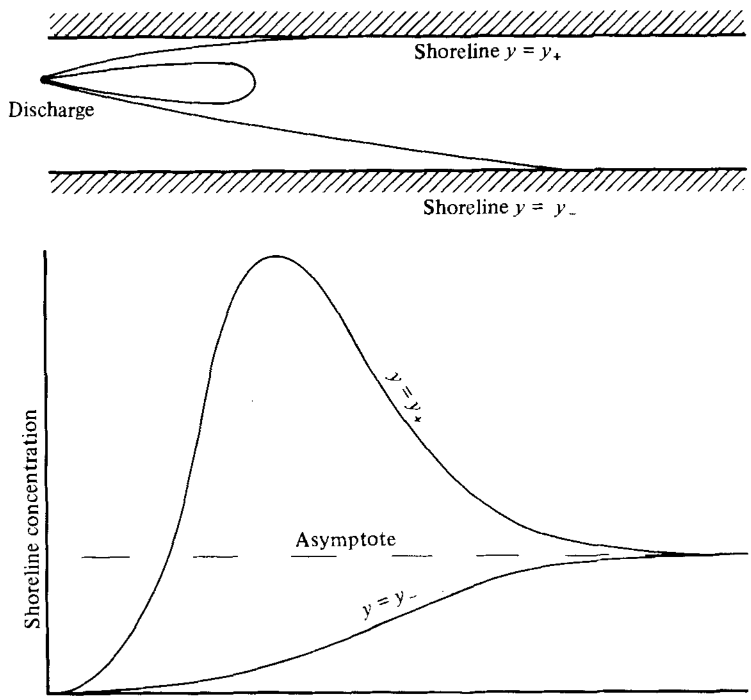

FIGURE 1. Sketch of a contaminant plume in a river, and the concentration at the two shorelines.

2. Transverse diffusion equation

In natural streams vertical mixing is achieved very much more rapidly than transverse mixing, i.e. 40 water depths as opposed to 100 channel breadths downstream (Smith 1979). Thus, when studying lateral mixing we can regard the contaminant concentration as being vertically well-mixed. The appropriate form of the advection–diffusion equation is therefore the depth-averaged equation

$$h\partial_t c + h(\mathbf{u}\,.\,\nabla)\,c = \nabla\,.\,(h\boldsymbol{\kappa}\,.\,\nabla c), \quad \text{with} \quad \nabla\,.\,(h\mathbf{u}) = 0, \tag{1a, b}$$

where h is the water depth, $\mathbf{u}$ the steady flow velocity, and $\boldsymbol{\kappa}$ the horizontal contaminant-dispersion tensor (which is assumed to incorporate cross-stream circulation as well as turbulence).

For steady discharges a second major simplification is that the contaminant plume is greatly elongated in the flow direction, i.e. by a factor of 100. Thus, we need only retain the cross-flow component of the diffusive flux $h\boldsymbol{\kappa}\,.\,\nabla c$. In a straight channel this leads to the equation

$$hu\,\partial_x c = \partial_y(h\kappa_{22}\partial_y c), \tag{2}$$

where x and y are the longitudinal and transverse co-ordinates. In a meandering stream it is first necessary to use a generalized co-ordinate system aligned along and across the depth-averaged flow (figure 2). The generalization of (2) is then

$$m_2 hu\,\partial_x c = \partial_y((m_1/m_2)\,h\kappa_{22}\partial_y c), \quad \text{with} \quad \partial_x(m_2 hu) = 0, \tag{3a, b}$$

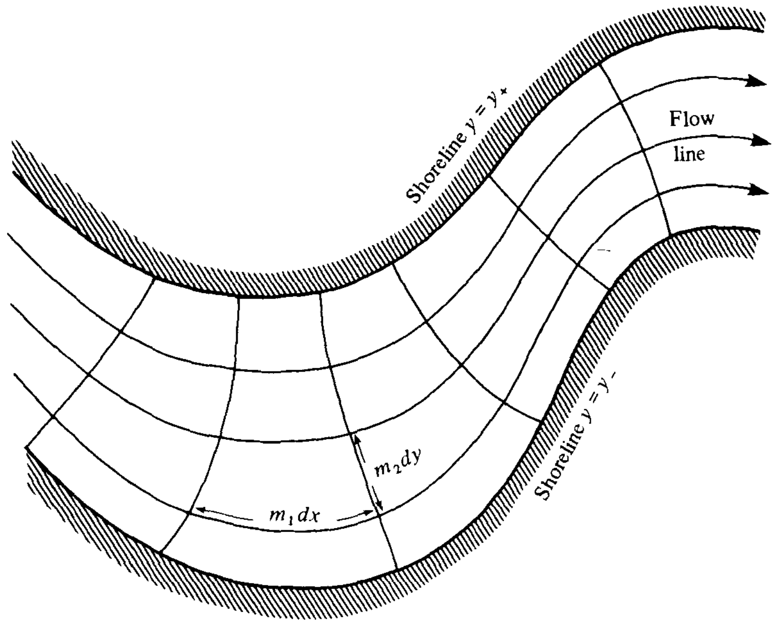

FIGURE 2. Orthogonal curvilinear co-ordinate system for a meandering stream.

where m_1, m_2 are the metric coefficients (Yotsukura & Sayre 1976). Provided that there is no horizontal re-circulation (e.g. embayments), the no-flux boundary conditions for (2, 3) are applied on lines of constant y:

$$(m_1/m_2)\, h\kappa_{22}\partial_y c = 0 \quad \text{on} \quad y = y_-, y_+. \tag{4}$$

3. Eigenfunction expansion

To solve (2) with the boundary conditions (4) we introduce the advection–diffusion eigenmodes $\phi_n(y)$:

$$\frac{d}{dy}\left(h\kappa_{22}\frac{d\phi_n}{dy}\right) + \mu_n hu\phi_n = 0, \tag{5a}$$

with

$$h\kappa_{22}\, d\phi_n/dy = 0 \quad \text{on} \quad y = y_-, y_+, \tag{5b}$$

$$\int_{y_-}^{y_+} hu\phi_n^2\, dy = Q = \int_{y_-}^{y_+} hu\, dy. \tag{5c}$$

The normalization (5c), in terms of the total volume flow rate Q, ensures that the lowest mode is

$$\phi_0 = 1 \quad \text{with} \quad \mu_0 = 0. \tag{6}$$

If the source distribution at $x = 0$ is denoted by $f(y)$, then the solution for $c(x, y)$ can be written

$$c = c_0 + \sum_{n=1}^{\infty} c_n \exp(-\mu_n x)\, \phi_n(y), \tag{7a}$$

with

$$c_n = \frac{1}{Q}\int_{y_-}^{y_+} huf\phi_n\, dy. \tag{7b}$$

To generalize this solution procedure to the case of meandering streams, we must incorporate the x-dependence of geometrical and flow properties m_1, m_2, h, u, κ_{22}. Instead of ($5a$–c) we now introduce the pair of adjoint advection–diffusion equations

$$m_2 hu\,\partial_x \phi_n = \partial_y((m_1/m_2)\,h\kappa_{22}\,\partial_y \phi_n) + \mu_n m_2 hu\phi_n, \tag{8a}$$

$$-m_2 hu\,\partial_x \hat{\phi}_n = \partial_y((m_1/m_2)\,h\kappa_{22}\,\partial_y \hat{\phi}_n) + \mu_n m_2 hu\hat{\phi}_n, \tag{8b}$$

with

$$h\kappa_{22}\partial_y \phi_n = h\kappa_{22}\partial_y \hat{\phi}_n = 0 \quad \text{on} \quad y = y_-, y_+, \tag{8c}$$

$$\int_{y-}^{y+} m_2 hu\phi_n \hat{\phi}_n\,dy = Q = \int_{y-}^{y+} m_2 hu\,dy, \tag{8d}$$

$$\int_{y-}^{y+} m_2 hu\hat{\phi}_n\,\partial_x \phi_n\,dy = \int_{y-}^{y+} m_2 hu\phi_n\,\partial_x \hat{\phi}_n\,dy = 0. \tag{8e}$$

It is this last constraint ($8e$) which minimizes the rate of change with respect to x, and ensures that the adjoint functions $\phi_n(x, y)$, $\hat{\phi}_n(x, y)$ become independent of x when the channel is uniform.

The generalization of the solution ($7a$, b) for the concentration distribution $c(x, y)$ is

$$c = c_0 + \sum_{n=1}^{\infty} c_n \exp\left(-\int_0^x \mu_n(x')\,dx'\right)\phi_n(x, y), \tag{9a}$$

with

$$c_n = \frac{1}{Q}\int_{y-}^{y+} m_2 huf\hat{\phi}_n\,dy. \tag{9b}$$

4. Avoiding the overshoot

At large distances downstream the approach to the asymptote will be dominated by the longest persisting mode. One characterization of the solutions to the Sturm–Liouville equations ($5a$–c) is in terms of increasing eigenvalues (Ince 1956, chap. 10)

$$0 < \mu_1 < \mu_2 < \dots. \tag{10}$$

Thus, unless $c_1 = 0$, ($7a$) yields

$$c \sim c_0 + c_1 \exp(-\mu_1 x)\,\phi_1(y) \quad \text{as} \quad x \to \infty. \tag{11}$$

A second characterization of the eigenfunctions $\phi_n(y)$ is in terms of their number n of zero crossings (see figure 3). The first non-constant eigenfunction $\phi_1(y)$ has a single zero y_1 and has opposite signs at the two banks y_-, y_+. Thus, unless $c_1 = 0$, the concentration (11) will exceed the asymptote at one side of the channel. The only way to avoid this overshoot is to enforce $c_1 = 0$. For a point discharge the only site that will achieve this condition is the single zero of $\phi_1(y)$:

$$\phi_1(y_1) = 0. \tag{12}$$

With c_1 identically zero the asymptote (11) needs to be replaced by

$$c \sim c_0 + c_2 \exp(-\mu_2 x)\,\phi_2(y) \quad \text{as} \quad x \to \infty. \tag{13}$$

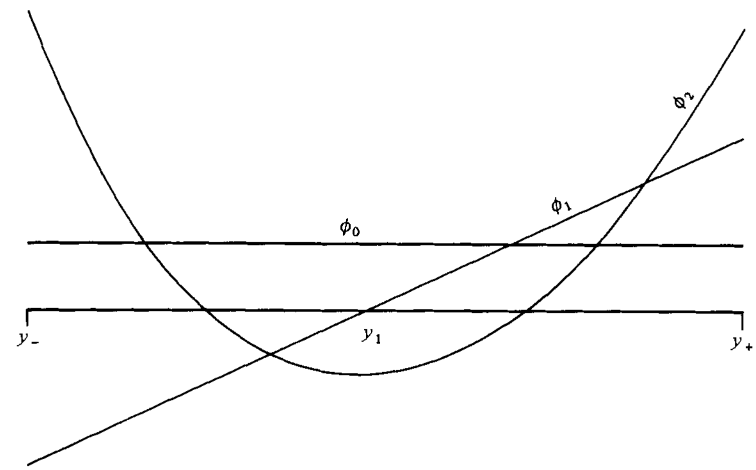

FIGURE 3. Sketch of advection–diffusion eigenmodes $\phi_n(y)$ showing their interlacing zeros.

The second non-constant eigenfunction $\phi_2(y)$ has the same sign at the two banks y_-, y_+ (see figure 3). Thus the presence or absence of overshoot depends upon the sign of the coefficient c_2. For a point discharge we have

$$c_2 = c_0\phi_2(y_1). \tag{14}$$

The zeros of successive eigenfunctions interlace. Hence, $\phi_2(y_1)$ is of the opposite sign to both $\phi_2(y_-)$ and $\phi_2(y_+)$. Consequently, the approach to the asymptote is from below at both banks, and the overshoot has been avoided.

For meandering channels the above argument goes through virtually unchanged, except that the definition of the optimal source position $y_1(x)$ becomes

$$\hat{\phi}_1(x, y_1) = 0. \tag{15}$$

The elimination of the most slowly decaying mode ϕ_1 in the concentration distribution ($7a$, $9a$) is quivalent to ensuring that complete mixing is achieved as quickly as possible. Thus, optimization with respect to shoreline concentrations yields the same discharge site as does optimization with respect to the degree of mixing (Yotsukura & Cobb 1972).

5. Straight channels

A simple but realistic model for the velocity and diffusivity distributions across a straight channel is

$$u = \bar{u}h^{\frac{1}{2}}\bar{h}/\overline{h^{\frac{3}{2}}}, \quad \kappa_{22} = \bar{\kappa}h^{\frac{3}{2}}\bar{h}/\overline{h^{\frac{5}{2}}} \tag{16a, b}$$

(i.e. with the cross-stream dispersion dominated by the turbulence contribution), where the overbars denote cross-sectional average values (Smith 1981a). Thus the eigenvalue problem ($5a$, b) becomes

$$\frac{d}{dy}\left(h^{\frac{5}{2}}\frac{d\phi_n}{dy}\right) + \mu_n\left(\frac{\bar{u}\,\overline{h^{\frac{5}{2}}}}{\bar{\kappa}\overline{h^{\frac{3}{2}}}}\right)h^{\frac{3}{2}}\phi_n = 0, \tag{17a}$$

with

$$h^{\frac{5}{2}}\,d\phi_n/dy = 0 \quad \text{on} \quad y = y_-, y_+. \tag{17b}$$

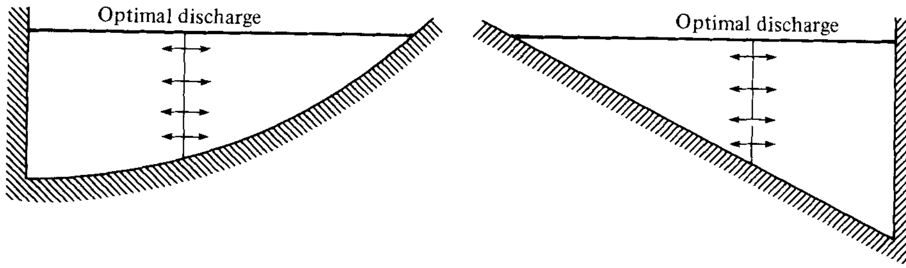

FIGURE 4. The positions of the optimal discharge sites in a semi-parabolic and in a triangular channel.

The normalization ($5c$) is no longer of importance, because we are only concerned to locate the zero-crossing y_1 of the first mode $\phi_1(y)$. For arbitrary depth profiles numerical methods would be required to determine this first eigenmode.

One depth profile for which ($17a, b$) can be solved analytically is the parabolic profile

$$h = H(1-(y/B)^2). \tag{18}$$

Depending upon whether the depth profile is symmetric, or only extends over the half-range $0 < y < B$, the eigenfunctions are Gegenbauer polynomials of degree n or $2n$:

$$\phi_n(y) = C_n^{(2)}(y/B) \quad \text{if} \quad y_- = -B, \quad y_+ = B, \tag{19a}$$

$$\phi_n(y) = C_{2n}^{(2)}(y/B) \quad \text{if} \quad y_- = 0, \quad y_+ = B \tag{19b}$$

(Abramowitz & Stegun 1964, chap. 22). At $n = 1$ we find that the optimal discharge sites are

$$y_1 = 0 \quad \text{for a symmetric channel}, \tag{20a}$$

$$y_1 = B\sqrt{\tfrac{1}{6}} \quad \text{for a semi-parabolic channel} \tag{20b}$$

(see figure 4).

Next, for a triangular channel

$$h = H(y/B) \quad (0 < y < B), \tag{21}$$

the eigenfunctions are

$$\phi_n = \frac{\sin(a_n(y/B)^{\frac{1}{2}})}{(a_n(y/B)^{\frac{1}{2}})^3} - \frac{\cos(a_n(y/B)^{\frac{1}{2}})}{(a_n(y/B)^{\frac{1}{2}})^2}, \tag{22a}$$

with

$$\tan a_n = 3a_n/(3-a_n^2). \tag{22b}$$

The first non-zero root is

$$a_1 = 5{\cdot}76. \tag{23}$$

For the eigenfunctions ϕ_n the zero-crossings arise when

$$\tan(a_n(y/B)^{\frac{1}{2}}) = a_n(y/B)^{\frac{1}{2}}. \tag{24}$$

In particular, the first zero is at

$$a_n(y/B)^{\frac{1}{2}} = 4{\cdot}49. \tag{25}$$

Combining the results (23, 25) we conclude that the optimal discharge site is

$$y_1 = 0{\cdot}607\,B \tag{26}$$

(see figure 4).

In both of the above examples the optimal discharge site is weighted towards the deeper part of the channel. The explanation is that contaminant plumes tend to curve towards the shallower water (Kay 1982; Smith 1981*b*). It is to counteract this tendency that the siting of the discharge must be weighted towards the deeper water.

6. A meandering channel

In a meandering channel the complexity of the flow field (Rozovskii 1961) and the strong dependence of the transverse-dispersion coefficient κ_{22} upon the flow curvature (Fischer 1969), means that there is no practical alternative but to solve (8*a–e*) numerically. However, it is enlightening to investigate an idealized case in which some of the general features of contaminant dispersion in meandering flows can be revealed analytically. To do this, we assume that the velocity, depth profile, and transverse diffusivity are independent of the longitudinal co-ordinate x. Also, we assume that the flow lines remain equispaced:

$$m_1 = 1 + y\rho(x), \quad m_2 = 1. \tag{27}$$

Thus, in the eigenfunction equations (8*a–e*) the x-dependence only arises via the changing curvature $\rho(x)$.

The deliberate resemblance to the straight-channel case permits us to make use of the normalized eigenmodes $\phi_n^{(0)}(y)$, where the zero superscript alludes to the zero value of the curvature. Thus, we pose the representations

$$\phi_1 = \phi_1^{(0)}(y) + \sum_{n=1}^{\infty} a_n(x)\,\phi_n^{(0)}(y), \tag{28a}$$

$$\hat{\phi}_1 = \phi_1^{(0)}(y) + \sum_{n=1}^{\infty} \hat{a}_n(x)\,\phi_n^{(0)}(y), \tag{28b}$$

$$\mu_1 = \mu_1^{(0)} + \eta(x). \tag{28c}$$

The $\phi_n^{(0)}$ components of (8*a, b*) yield ordinary differential equations for the coefficients $a_n(x), \hat{a}_n(x)$:

$$\partial_x a_1 = \eta + \rho(x)\,Y_{11} + \eta a_1 + \rho(x) \sum_{j=1}^{\infty} a_j Y_{1j}, \tag{29a}$$

$$\partial_x a_n = -(\mu_n^{(0)} - \mu_1^{(0)})\,a_n + \rho(x)\,Y_{1n} + \eta a_n + \rho(x) \sum_{j=1}^{\infty} a_j Y_{jn}, \tag{29b}$$

$$-\partial_x \hat{a}_1 = \eta + \rho(x)\,Y_{11} + \eta \hat{a}_1 + \rho(x) \sum_{j=1}^{\infty} \hat{a}_j Y_{1j}, \tag{29c}$$

$$-\partial_x \hat{a}_n = -(\mu_n^{(0)} - \mu_1^{(0)})\,\hat{a}_n + \rho(x)\,Y_{1n} + \eta \hat{a}_n + \rho(x) \sum_{j=1}^{\infty} \hat{a}_j Y_{jn}, \tag{29d}$$

with

$$Y_{nj} = Y_{jn} = \frac{1}{Q}\int_{y_-}^{y_+} \mu_j^{(0)}\, hu\phi_j^{(0)} \left[\int_0^{y} \phi_n^{(0)}\,dy' - y\phi_n^{(0)}\right] dy. \tag{29e}$$

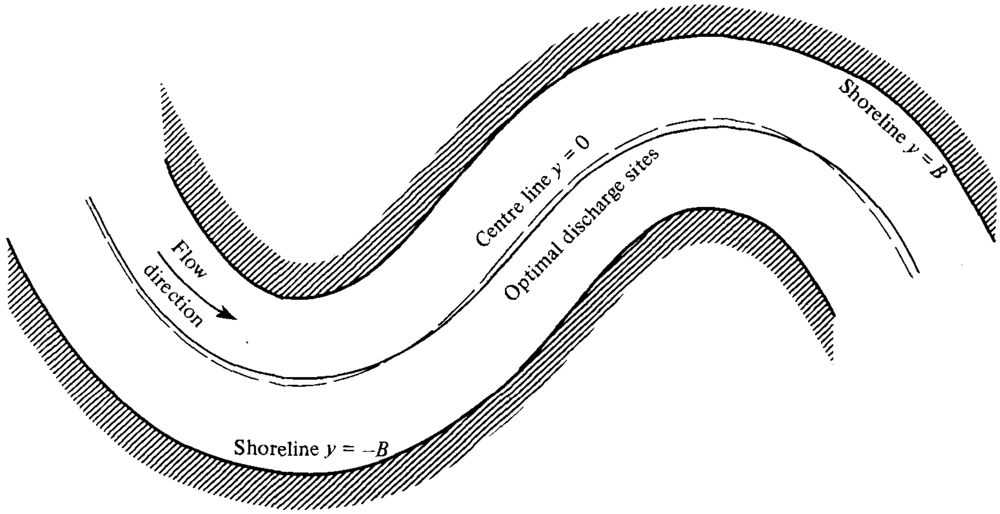

FIGURE 5. The optimal discharge site in a meandering river of parabolic cross-section.

The constraint (8*e*) takes the form

$$\partial_x a_1 + \sum_{n=1}^{\infty} \hat{a}_n \partial_x a_n = \partial_x \hat{a}_1 + \sum_{n=1}^{\infty} a_n \partial_x \hat{a}_n = 0, \tag{30}$$

and can be transformed into an equation for $\eta(x)$:

$$\eta\{1 + a_1 + \hat{a}_1 + \sum_{n=1}^{\infty} a_n \hat{a}_n\} = \rho Y_{11} + \sum_{n=1}^{\infty} (\mu_n^{(0)} - \mu_1^{(0)})\, a_n \hat{a}_n + \rho \sum_{n=1}^{\infty} Y_{1n}(a_n + \hat{a}_n) + \rho \sum_{n=1}^{\infty} \sum_{j=1}^{\infty} Y_{nj} a_n \hat{a}_j. \tag{31}$$

The coupling between the equations (29*a*–*d*) is quadratic in the variables ρ, η, a_j, $\hat{a}_j$. Thus, if the bends are not too severe, then we can neglect the coupling and the equations can be solved explicitly:

$$a_1 = 2Y_{11} \int_0^{\infty} \rho(x - x')\, dx', \tag{32a}$$

$$a_n = Y_{1n} \int_0^{\infty} \exp\left(-(\mu_n^{(0)} - \mu_1^{(0)})\, x'\right) \rho(x - x')\, dx', \tag{32b}$$

$$\hat{a}_1 = 2Y_{11} \int_0^{\infty} \rho(x + x')\, dx', \tag{32c}$$

$$\hat{a}_n = Y_{1n} \int_0^{\infty} \exp\left(-(\mu_n^{(0)} - \mu_1^{(0)})\, x'\right) \rho(x + x')\, dx'. \tag{32d}$$

The optimal discharge position $y_1(x)$ is along the zero contour of $\hat{\phi}_1(x, y)$. From (28*b*) we infer that the first dependence of $y_1(x)$ upon curvature arises at a_2. Thus, it is the curvature over a distance of order $1/(\mu_2^{(0)} - \mu_1^{(0)})$ downstream of the source that determines the optimal location. The relative shapes of $\phi_1^{(0)}$, $\phi_2^{(0)}$ (see figure 3) enable us to infer that the displacement of $y_1(x)$ is always towards the inside of the bend. This

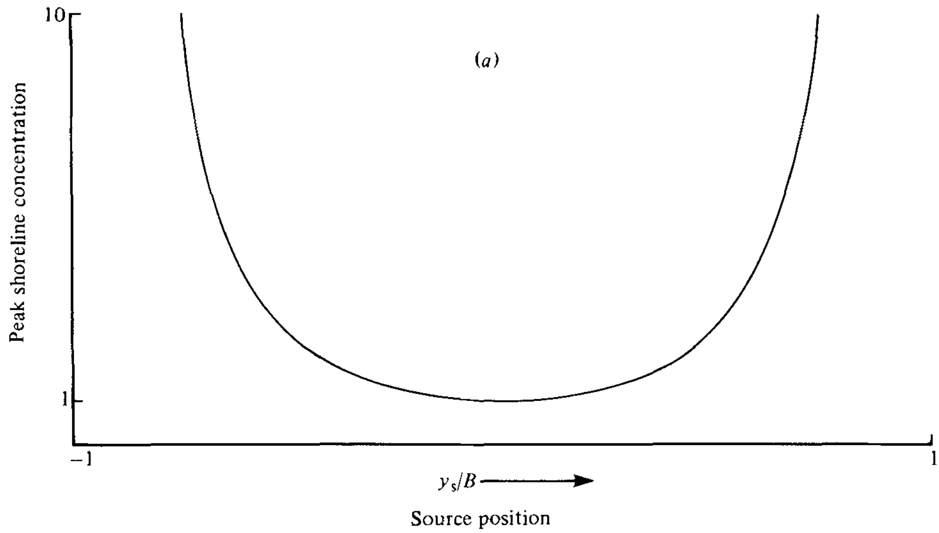

FIGURE 6. (*a*) For legend see p. 10.

can be thought of as counteracting the tendency for a contaminant plume to move towards the outside of bends (Ward 1974, figure 7; Smith 1981*b*, figure 4).

As an explicit example, we take the depth profile to be a symmetric parabola (18) with the velocity distribution and transverse diffusivity given by (16*a*, *b*). The normalized eigenfunctions are

$$\phi_n^{(0)}(y) = (3/(n+1)(n+3))^{\frac{1}{2}} C_n^{(2)}(y/B), \tag{33a}$$

with

$$\mu_n^{(0)} = \tfrac{6}{5}n(n+4)(\bar{\kappa}/\bar{u}B^2). \tag{33b}$$

Conveniently, the Y_{1n} coefficients are all zero with the sole exception of Y_{12}:

$$Y_{12} = -3(\tfrac{6}{5})^{\frac{1}{2}}(\bar{\kappa}/\bar{u}B). \tag{34}$$

If the curvature varies sinusoidally,

$$\rho(x) = \rho_0 \sin lx, \tag{35}$$

then the resulting formula for $\hat{\phi}_1(x, y)$ is

$$\hat{\phi}_1 = 6^{\frac{1}{2}}\left\{(y/B) - \frac{1}{5}\frac{\rho_0 B(1-6(y/B)^2)}{1+(l\bar{u}B^2/6\bar{\kappa})^2}[\sin lx + (l\bar{u}B^2/6\bar{\kappa})\cos lx]\right\}. \tag{36}$$

Figure 5 shows how the displacement of y_1 leads the changing sign of the curvature for the specific case

$$\rho_0 B = \tfrac{1}{2}, \quad lB = \tfrac{1}{2}, \quad \bar{\kappa}/\bar{u}B = \tfrac{1}{12}. \tag{37}$$

7. Non-optimal discharges

In practice, the cost of using an optimal discharge site in relatively deep water, rather than a site closer to the bank, is justifiable only if there is a significant reduction in the pollution levels. Since the optimal site gives a minimum for the peak shoreline

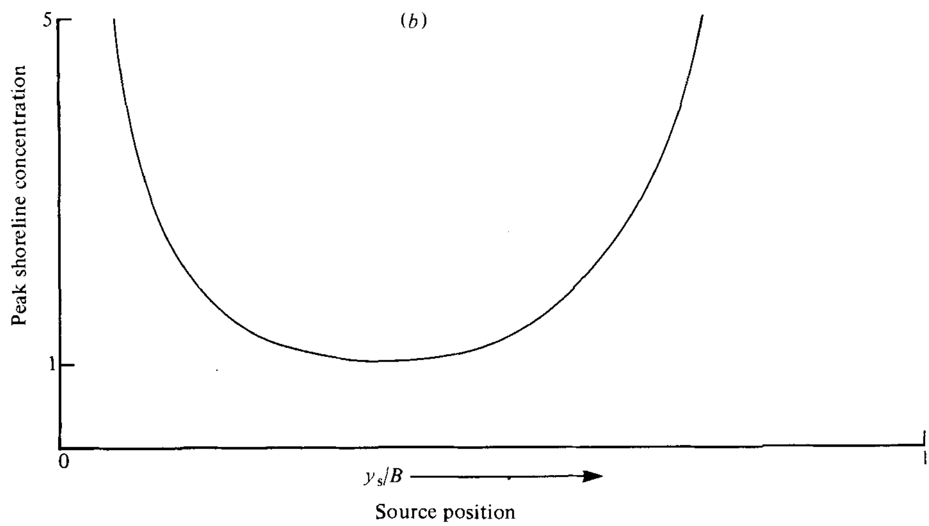

FIGURE 6. The peak shoreline concentration for different discharge sites across symmetric and semi-parabolic channels.

concentration, nearby sites will give almost unchanged results. Thus, the key question becomes how flat is the minimum.

For a straight channel the coefficients c_n in the eigenfunction expansion (7a) are given by

$$c_n = c_0 \phi_n(y_s), \tag{38}$$

where y_s is the source position and ϕ_n the nth normalized eigenmode. Once c_n and the decay rates μ_n are known it is a straightforward numerical task to evaluate the shoreline concentration and to find its peak value. Figures 6(a, b) show the results for symmetric and semi-parabolic channels. Either side of the optimal site there is a region of about a quarter of the total channel breadth in which the peak concentration is within a factor of two of its minimum value. However, there is an alarmingly high increase in pollution levels if the discharge site is chosen to be even further away from its optimal location.

The financial support of the Royal Society and British Petroleum is gratefully acknowledged.

REFERENCES

ABRAMOWITZ, M. & STEGUN, I. A. 1964 *Handbook of Mathematical Functions*. Dover.

FISCHER, H. B. 1969 The effect of bends on dispersion in streams. *Water Resources Res.* **5**, 496–506.

INCE, E. L. 1956 *Ordinary Differential Equations*. Dover.

KAY, A. 1982 The effect of a sharp cross-stream depth change upon contaminant dispersion in a vertically well-mixed current. *J. Hydraul. Div. A.S.C.E.* (submitted).

ROZOVSKII, I. L. 1961 *Flow of Water in Bends of Open Channels* (transl. from 1957 Russian edn). OTS60-5113, Department of Commerce, Washington, D.C.

SMITH, R. 1979 Calculation of shear-dispersion coefficients. In *Mathematical Modelling of Turbulent Diffusion in the Environment* (ed. C. J. Harris), pp. 343–362. Academic.

SMITH, R. 1981*a* The importance of discharge siting upon contaminant dispersion in narrow rivers and estuaries. *J. Fluid Mech.* **108**, 43–53.

SMITH, R. 1981*b* Effect of non-uniform currents and depth variations upon steady discharges in shallow water. *J. Fluid Mech.* **110**, 373–380.

WARD, P. R. B. 1974 Transverse dispersion in oscillatory channel flow. *J. Hydraul. Div. A.S.C.E.* **100**, 755–772.

YOTSUKURA, N. & COBB, E. D. 1972 Transferse diffusion of solutions in natural streams. *U.S. Geo. Survey Paper*, no. 582-C.

YOTSUKURA, N. & SAYRE, W. W. 1976 Transverse mixing in natural channels. *Water Resources Res.* **12**, 695–704.